Influence of Short Chain Branching on the Miscibility of Binary Polymer Blends: Application to Polyolefin Mixtures

Karl F. Freed and Jacek Dudowicz*

The James Franck Institute and the Department of Chemistry, University of Chicago, Chicago, Illinois 60637

Received July 24, 1995; Revised Manuscript Received October 23, 1995[⊗]

ABSTRACT: The lattice cluster theory (LCT) is used to study the influence of monomer structure, i.e., short chain branching, on the miscibility of binary polymer blends. The systems are chosen as corresponding to united atom models of the monomer structures in the binary polyolefin blends studied by Graessley and co-workers. We focus on the short chain branching by using a compressible blend model with a single interaction energy for all united atom groups. The polyolefin blend miscibilities are found to correlate well with a monomer structure dependent branching parameter r, the excess volume, and the SANS interaction parameter χ_{eff}. Our calculations also demonstrate that except for very immiscible polyolefin blends both the "entropic" and "enthalpic" portions of χ_{eff} are relevant and comparable to each other, with an increasing dominance of the entropic part over the enthalpic contribution when the blend miscibility improves. Computations are also provided for the pressure dependence of the blend miscibilities. Solubility parameters and stiffness asymmetries do not correlate with our computed blend miscibilities. Although quantitative comparisons with experiment will at least require the use of monomer dependent interaction energies, the present LCT computations permit us to understand certain experimental trends.

I. Introduction

The recent development of metallocene catalysts for polyolefin production promises to revolutionize the ability of tailoring polyolefins into thermoplastic elastomers that will likely replace the engineering polymers currently used in transportation. The new catalysts produce random copolymers as opposed to the older kinetically controlled ones that tend to have higher degrees of short chain branching in the lower molecular weight components. Thus, the new catalysts enable controlling the sizes of the crystalline and rubbery domains and, hence, the properties of the materials.

A series of experiments by Graessley and co-workers[1−4] has sought to understand the physics governing the miscibility of polyolefins. Their work indicates a rough correlation between the patterns of miscibility and the solubility parameters determined either from small angle neutron scattering or equation of state experiments. However, several systems exhibit departures from this simple theory, especially those containing poly(isobutylene) (PIB), and have lower critical solution temperature phase diagrams. The origins of these deviations from the solubility parameter theory, and hence, from the Berthelot combining rule,[5] remain unknown. However, it may be surmised that the explanation of these deviations should greatly expand our understanding of the factors influencing blend miscibility, thereby contributing to the goal of designing new high-performance materials.

Bates, Fredrickson, and co-workers[6] have proposed a relation between blend miscibility and the asymmetry in local chain stiffness of the individual blend components. Their approach is simply based on a combination of incompressible Flory−Huggins (FH) theory with the contribution to the free energy from the Gaussian fluctuations as calculated using the incompressible random phase approximation. The theory[6] represents the Flory interaction parameter χ in terms of differences of Kuhn segment lengths, ascribing the miscibility patterns observed in polyolefins to purely entropic factors associated with Kuhn length asymmetries between the blend components. (Small enthalpic contributions may arise from the temperature dependence of the Kuhn lengths.) Graessley and co-workers do find[2] some agreement between their patterns of blend miscibility and those predicted on the basis of the Bates−Fredrickson theory, but the solubility parameter treatment yields a superior, but still not totally adequate, description.

Singh and Schweizer[7] have sought to obtain a more molecular understanding of both the Bates−Fredrickson theory and of the experimental polyolefin data by using integral equation PRISM computations. They model the two blend components as linear chains with different degrees of bond angle bending stiffness, a model designed to mimic on a more molecular level the model of Bates, Fredrickson and co-workers. The PRISM computations consider athermal models that are the analogs of the Bates−Fredrickson model, as well as models containing the monomer−monomer interaction energies. The near chemical identity of the polyolefin units leads Singh and Schweizer[7] to study simple models in which all the units on the chains of both species interact with the same interaction potential. The PRISM computations indicate that the polyolefin blend miscibility is dominated by enthalpic interactions, with much smaller entropic contributions to χ. The importance of enthalpic interactions in a system with equal attractive interaction potentials may be understood to emerge because the PRISM calculations contain the realistic feature of the presence of excess free volume.[8,9] This excess free volume acts as a noninteracting, nonselective solvent whose affinity for the blend components is influenced by what has loosely been associated with the "polymer surface fraction",[10,11] which must be different for the two blend components.[11] Both the Bates−Fredrickson theory and the solubility parameter analyses consider incompressible blend models and, therefore, do not contain the extra contribution, due to the presence of excess free volume, that is obtained from the PRISM calculations and that has been demonstrated using the lattice cluster

[⊗] Abstract published in *Advance ACS Abstracts,* December 1, 1995.

0024-9297/96/2229-0625$12.00/0

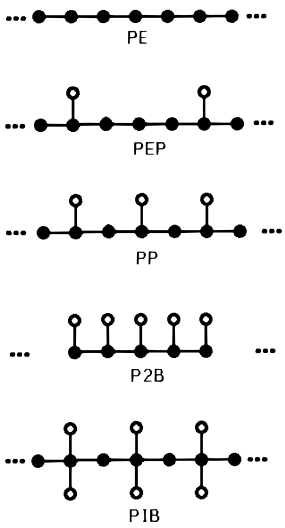

Figure 1. United atom models for portions of polyethylene (PE), poly(ethylpropylene) (PEP), polypropylene (PP), poly(2-butene) (P2B), and polyisobutylene (PIB) chains. Circles denote CH_n ($n = 0-3$) groups occupying single lattice sites. Filled circles indicate the backbone chain groups, while open ones are for the side groups.

theory[12] (LCT) to exert a significant influence upon the temperature, composition, molecular weight, and pressure dependence of χ.[13-17] Thus, we concur with Schweizer and co-workers on the importance of using a compressible model for describing the polyolefin blends, a model that, of necessity, introduces important enthalpic contributions to χ.

Since the lattice cluster theory does not currently treat bending energies and, consequently, cannot yet consider the lattice analog of the model used by Singh and Schweizer, we focus upon a different type of analysis for the factors influencing polyolefin blend miscibilities. We investigate how short chain branching affects blend miscibility, a technologically important phenomenon which is poorly understood and only recently studied by considering more complex random copolymer systems.[1-4] The influence of short chain branching in polyolefin blends may be described with the LCT by using united atom models for the polyolefin chains. These united atom models take each CH_n united atom group (for $n = 0, 1, ..., 3$) to reside on a single lattice site. The individual monomers cover several lattice sites, as dictated by their molecular structures. (See Figure 1 for several examples.) The bonds between united atom units are completely flexible, but the excluded volume prohibition of multiple occupancy of any lattice site and the treatment of local correlations by the LCT both conspire to introduce a measure of stiffness into the LCT description of polymers with structured monomers. Thus, we may also investigate the existence of any correlations between the LCT computations of blend miscibility and this chain stiffness. However, we choose to focus primarily on the very important influence of the monomer structure with its short chain branching. This focus is consistent with our desire for a deeper molecular understanding of blend miscibilities.

The chemical similarity of the different united atom units in polyolefins leads us further to introduce, as a first approximation, a compressible blend model in which all united atom units interact by the same microscopic energy ϵ with united atom units of either chain species that occupy nearest neighbor lattice sites. This feature of our model accords with that of Singh and Schweizer[7] since the creation of excess free volume in the blend removes contacts between united atom subgroups, thereby providing an enthalpic contribution to the free energy and, hence, possibly affecting the blend miscibility, in spite of the vanishing of the exchange energy, $\epsilon_{ex} = \epsilon_{11} + \epsilon_{22} - 2\epsilon_{12} = 0$. However, it should be noted from the outset that the different CH_n united atom units (for $n = 0, 1, ..., 3$) *must* have different van der Waals interaction energies $\epsilon_{nn'}$. For example, standard Lennard-Jones potentials for united atom models of alkanes[18] have $\epsilon_{CH_3-CH_3} = 90$ K for the interaction of a pair of CH_3 units, but only $\epsilon_{CH_2-CH_2} = 70$ K for the CH_2 units. Flory's classic description[19] of the thermodynamics of alkane mixtures uses a treatment that loosely corresponds to a fluid of CH_2 and CH_3 units that interact with different van der Waals energies. Thus, we must emphasize that although our molecular model represents a sensible first approximation for investigating the influences of short chain branching, the model omits contributions from interaction asymmetries in order to isolate the influences of short chain branching. The experiments of Graessley and co-workers find[4] the greatest deviations from the solubility parameter theory and, hence, from a random mixing model as arising from blending two polyolefins whose equations of state have rather different reduced temperatures T^*. The rough correspondence between T^* for a melt and the microscopic interaction ϵ between subunits of the chain is a strong indication for the ultimate necessity of including these differences by introducing a set of species dependent $\{\epsilon_{nn'}\}$. The LCT is, indeed, designed to treat interactional asymmetries,[12] but computations containing both these asymmetries and the monomer molecular structures would have both sets of effects inexorably intertwined. Section IV does, however, discuss some general implications of the presence of different interaction energies and how these differences may explain some experimental findings. We leave for a future study LCT computations with different interaction energies since this future study will first require the tedious process of fitting some pure component interaction energies to PVT data and then fitting heterocontact interaction energies to binary blend data.[17] Thus, this quantitative comparison with experiment is planned to follow the present more qualitative investigation of how short side group branching affects the miscibility of binary polyolefin blends.

Section II briefly sketches the LCT-generalized united atom lattice model for polyolefin chains, the assumptions and content of the LCT, the constant pressure stability conditions, the definition of the effective interaction parameter χ_{eff}, and the LCT equation for the relative excess volume $V^e/(V_1 + V_2)$ of a binary blend. Section III summarizes the LCT computations of the phase diagrams and describes correlations between the blend miscibility and other thermodynamic quantities [such as χ_{eff} or $V^e/(V_1 + V_2)$] of polyolefin blends, as well as a blend branching parameter r which is a measure of blend structural asymmetry. This parameter r contains more detailed information concerning the chain structure than provided by the common measure of polymer similarity given by the ratio of end groups to total groups in the chain. Section IV considers correlations with structural parameters, such as solubility parameters and chain stiffness, and discusses likely physical origins for the discrepancies found by Graessley et al.[2,4] between solubility parameter theory predictions and blend miscibility.

II. Lattice Cluster Theory of a Binary Blend

A. Model of a Binary Blend with Identical Monomer−Monomer Interactions. The extended lattice model of a binary blend represents each component α (α = 1 and 2) as n_α monodisperse polymer chains placed on a regular array of N_l lattice sites and coordination number z. A single chain of species α occupies $M_\alpha = N_\alpha s_\alpha$ lattice sites, where N_α is the polymerization index and s_α designates the number of lattice sites covered by a single monomer of species α. In contrast to the standard lattice model, the monomer occupancy index s_α is no longer forced to equal unity and may, in general, take any value necessary for realistically describing the monomer size and shape. The monomer structure is chosen for the polyolefins as corresponding to a united atom model in which individual united atom groups CH_n, for $n = 0$, 1, 2, or 3, reside at single lattice sites. The bonds between united atom groups correspond to C−C bonds. Figure 1 depicts the structures for the five model polyolefin chains considered in the present LCT computations. These models represent homopolymer analogs for the majority of the systems studied by Graessley and co-workers.[1−4]

The non-zero blend compressibility implies the existence of excess free volume which is modeled in the LCT by the presence of n_v empty sites (voids) with volume fraction $\phi_v = n_v/N_l$. The void volume fraction ϕ_v is determined from the equation of state for a given pressure, temperature, blend composition, and unit cell volume. The composition of the binary blend is expressed in terms of the nominal volume fractions $\Phi_1 = 1 - \Phi_2 = n_1M_1/(n_1M_1 + n_2M_2)$ which are simply related to the actual volume fractions $\phi_\alpha \equiv n_\alpha M_\alpha/N_l$ (useful only within a lattice model) by $\Phi_\alpha = \phi_\alpha/(1 - \phi_v)$. The lattice is assumed to be a three-dimensional ($d = 3$) cubic lattice with $z = 2d = 6$.

As for small molecule fluids, the interactions in polymer blends involve short range repulsions and longer range attractions. The former are naturally represented in the lattice model by excluded volume constraints that prohibit the double occupancy of any lattice site, while the latter are introduced by ascribing the attractive microscopic van der Waals energy $\epsilon_{\alpha\beta}^{i,j}$ to nearest neighbor (on the lattice) portions i and j of monomers α and β. All the s_α portions of a monomer α are taken as energetically equivalent units, which interact with any of the s_β portions of a monomer β with the same energy $\epsilon_{\alpha\beta}$. In addition, as the simplest model for studying the influence of short branches on blend miscibility, the three independent interaction energies ϵ_{11}, ϵ_{22}, and ϵ_{12} are assumed to be identical. This simple model forces the exchange energy $\epsilon_{ex} \equiv \epsilon_{11} + \epsilon_{22} - 2\epsilon_{12}$ to vanish identically. Incompressible Flory−Huggins theory would then imply $\chi_{FH} \equiv 0$, corresponding to a purely athermal system with complete miscibility. A compressible system with $\epsilon_{ex} \equiv 0$, on the other hand, is not athermal and may yield enthalpic contributions to the free energy as explained in the Introduction.[8,9] The choice of $\epsilon_{ex} \equiv 0$ enables the focus to be entirely on how branching and architecture affect the thermodynamic properties of binary polyolefin blends. Previous LCT computations[13−17] have been performed with three independent $\epsilon_{\alpha\beta}$ and could readily be applied here. However, such three-parameter LCT computations would involve an admixture of the influences of energetic asymmetries and short chain branches and are therefore best deferred to subsequent studies which would require a more laborious determination of the pure component $\epsilon_{\alpha\alpha}$ from melt equation of state data. (See ref 17 for examples of this procedure.) Since actual liquids at ambient pressures are liquids by virtue of the attractive interactions, the above simplified model is preferable to the often used highly unrealistic athermal limit models in which attractive interactions are entirely neglected.

B. Free Energy of a Binary Blend. The lattice cluster theory[12] (LCT) yields the Helmholtz free energy F of a binary blend in the form

$$\frac{F}{N_l k_B T} = \phi_v \ln \phi_v + \sum_{i=1}^{i=2} \frac{\phi_i}{M_i} \ln \frac{2\phi_i}{M_i} - (\ln z - 1) \sum_{i=1}^{i=2} \left(1 - \frac{1}{M_i}\right) \phi_i + \sum_{k=1}^{k^*} \sum_{l=0}^{k} f_{kl} \phi_1^{\,l} \phi_2^{\,k-l} \quad (2.1)$$

The first three terms on the right hand side of eq 2.1 provide the combinatorial part of F, while the last term represents the noncombinatorial portion as a polynomial in the actual volume fractions ϕ_1 and ϕ_2. The coefficients f_{kl} in eq 2.1 are generated as double expansions in the inverse lattice coordination number $1/z$ and in the three dimensionless microscopic van der Waals attractive energies $\epsilon_{\alpha\beta}/k_BT$, as described in a series of our papers.[12−17] The structure and molecular weight dependence of the free energy F enters solely through the coefficients in these double expansions. The present calculations of F are performed through orders $1/z^2$ and $(\epsilon_{\alpha\beta}/k_BT)^2$. This approximation fixes[12] the upper limit of k in the double summation in (2.1) as $k^* = 6$.

Polymer blends at constant pressure P are more appropriately described by the Gibbs free energy G,

$$G = F + PV = F + PN_l v_{cell} \quad (2.2)$$

The pressure P is computed from eq 2.1 as

$$P \equiv -\left.\frac{\partial F}{\partial V}\right|_{T,n_1,n_2} = -\frac{1}{v_{cell}} \left.\frac{\partial F}{\partial n_v}\right|_{T,n_1,n_2} \quad (2.3)$$

where the volume v_{cell} associated with one lattice site is assumed to be a constant. Equations 2.3 and 2.1 automatically produce the equation of state $P = P(\Phi_1,\phi_v,T,v_{cell})$, which enables ϕ_v to be determined as a function of Φ_1, T, and v_{cell}. Both the free energies G and F as well as the void volume fraction ϕ_v are practically insensitive to the choice of v_{cell} over wide ranges of pressures and temperatures. The different polyolefins are assumed, again for simplicity, to have the same v_{cell}. More general treatments of species dependent v_{cell} are possible, as discussed in ref 17, and are appropriate when used in conjunction with computations employing three different $\epsilon_{\alpha\beta}$ for a binary blend.

C. Stability of a Binary Blend at Constant Pressure. Generally, a binary system at constant pressure P and temperature T is stable (or metastable) if

$$\left.\frac{\partial^2 g}{\partial X_1^{\,2}}\right|_{P,T} > 0 \quad (2.4)$$

where g designates the specific Gibbs free energy and X_1 denotes a composition variable normalized such that $X_1 + X_2 = 1$. Standard thermodynamic analysis shows that the normalization of g and the choice of X_1 must be conjugate.[20] Since the polymer blend compositions are represented here in terms of the nominal volume

fractions,

$$\Phi_i = n_i M_i/(n_1 M_1 + n_2 M_2) = n_i M_i/N_{\rm occ} \qquad (2.5)$$

the free energy g used in the constraint of eq 2.4 must be expressed per occupied lattice site, i.e., $g = G/N_{\rm occ}$. Equating the left-hand side of the inequality (2.4) to zero and specifying the variable X_1 as Φ_1 produces the stability limit (called the "spinodal") for the constant pressure binary polymer blend,

$$\left.\frac{\partial^2 g}{\partial \Phi_1^{\,2}}\right|_{P,T} = 0 \qquad \text{(spinodal)} \qquad (2.6)$$

The condition of eq 2.6 may be converted into a more computationally convenient form,

$$\left.\frac{\partial \mu_{\rm ex}}{\partial \Phi_1}\right|_{P,T} = 0 \qquad (2.7)$$

by introducing the exchange chemical potential $\mu_{\rm ex} \equiv \mu_1 - \mu_2$, where the chemical potentials μ_1 and μ_2 are defined on a per lattice site basis as

$$\mu_i = \frac{1}{M_i}\left.\frac{\partial F}{\partial n_i}\right|_{V,T,n_{j\neq i}} = \left.\frac{\partial [F/N_1]}{\partial \phi_i}\right|_{N_1,T,\phi_{j\neq i}} \qquad i = 1 \text{ and } 2 \qquad (2.8a)$$

$$= \frac{1}{M_i}\left.\frac{\partial G}{\partial n_i}\right|_{P,T,n_{j\neq i}} \qquad (2.8b)$$

Since the derivatives $\partial\mu_1/\partial\Phi_1$ and $\partial\mu_2/\partial\Phi_1$ of eq 2.7 are related to each other through the Gibbs−Duhem equation,

$$\Phi_1 \left.\frac{\partial \mu_1}{\partial \Phi_1}\right|_{P,T} + \Phi_2 \left.\frac{\partial \mu_2}{\partial \Phi_1}\right|_{P,T} = 0 \qquad (2.9)$$

eq 2.7 further simplifies to

$$\left.\frac{\partial \mu_1}{\partial \Phi_1}\right|_{P,T} = 0 \qquad (2.10)$$

where the constant pressure derivative $\partial\mu_1/\partial\Phi_1$ is calculated from the LCT free energy expansion (2.1) along the lines derived previously by us.[21] The treatment of constant pressure coexistence curves is numerically much more tedious than the determination of stability boundaries, so such a computation is deferred to a future work on the interfacial properties of the polyolefin blends. The general trends for the coexistence curves parallel those for the spinodals presented here.

D. Small Angle Neutron Scattering Interaction Parameter $\chi_{\rm eff}$. The small angle neutral scattering effective Flory interaction parameter $\chi_{\rm eff}$ is a central quantity in theories of polymer fluids. Within the extended lattice model of binary blends, $\chi_{\rm eff}$ is generally defined in conjunction with small angle neutral scattering experiments as,

$$\chi_{\rm eff} = -\frac{1}{2}\left[\frac{1}{S(0)} - \frac{1}{M_1\Phi_1} - \frac{1}{M_2\Phi_2}\right] \qquad (2.11)$$

where $S(0)$ represents the extrapolated zero angle neutron scattering function (expressed on a per lattice site basis), the M_α denote individual chain site occupancy indices, and the Φ_α designate the nominal volume fractions which satisfy the condition $\Phi_1 + \Phi_2 = 1$. When the scattering is dominated by a single polymer species, say species 1, $S(0)$ reduces to $S(0) = S_{11}(0)$. (Reference 15 considers $S(0)$ for cases with incomplete contrast.) The zero wave vector partial structure factor $S_{11}(0)$ is related to the chemical potential μ_1 of eqs 2.8 by

$$S_{11}(0)^{-1} = \frac{n_1 M_1 + n_2 M_2}{M_2 k_{\rm B} T}\left.\frac{\partial \mu_1}{\partial n_2}\right|_{T,V,\mu_2} \qquad (2.12)$$

The absence of the occupancy index M_1 in the denominator of the prefactor in eq 2.12 arises from the normalization of the chemical potential μ_1 on a per lattice site basis (see eqs 2.8).

Another way of defining the effective interaction parameter is based on the application of the standard formula commonly used in the analysis of experimental SANS data,

$$\frac{k_N}{I(0)} = \frac{1}{N_1 v_1 \Phi_1} + \frac{1}{N_2 v_2 \Phi_2} - 2\frac{\chi_{\rm eff}'}{v_{\rm o}} \qquad (2.13)$$

where $I(0)$ is the absolute scattering intensity, v_1 and v_2 are the monomer molar volumes for species 1 and 2, respectively, $v_{\rm o}$ is an arbitrarily normalizing volume, often taken as $v_{\rm o} = (v_1 v_2)^{1/2}$, and k_N involves the scattering contrast. Both the absolute scattering intensity $I(0)$ and the structure factor $S(0)$ may be determined from the LCT provided that the free energy expansion of eq 2.1 is known.[17] Since our goal lies in studying the qualitative influence of short chain branching in polymer chains on blend thermodynamic properties rather than in detailed quantitative comparisons with experimental data, the computations of the interaction parameter are performed with the simpler definition in eq 2.11. Rather minor differences would emerge from using eq 2.13 instead.

E. Excess Volume of a Binary Blend at Constant Pressure. The excess volume $V^{\rm e} \equiv \Delta V = V_{\rm blend} - V_1 - V_2$ for a binary blend is the difference between the blend volume $V_{\rm blend}$ and the sum of the volumes V_1 and V_2 for the pure components that are mixed (at constant temperature and pressure) to produce the blend. Under the assumption of equal cell volumes for both pure component melts and the blend, the appropriate formula for the relative excess volume is given by

$$\frac{\Delta V}{V_1 + V_2} = \frac{1}{\dfrac{\Phi_1(1-\phi_{\rm v})}{1-\phi_{\rm v}^{(1)}} + \dfrac{\Phi_2(1-\phi_{\rm v})}{1-\phi_{\rm v}^{(2)}}} - 1 \qquad (2.14)$$

where Φ_1 and Φ_2 are the nominal volume fractions in the blend, while $\phi_{\rm v}$ and $\phi_{\rm v}^{(\alpha)}$ denote, respectively, the excess free volume fractions in the blend and in the pure melt of species α at the same pressure P and the temperature T.

III. LCT Computations

A series of LCT computations is performed for the spinodal curves $T = T(\Phi_1)$, the relative excess volume $V^{\rm e}/(V_1 + V_2)$, and the SANS effective interaction parameter $\chi_{\rm eff}$. These computations are applied to model binary polyolefin blends composed of all pairs of the five polymer species depicted in Figure 1. These species represent the united atom molecular structures for chains of polyethylene (PE), poly(ethylpropylene) (PEP), polypropylene (PP), poly(2-butene) (P2B), and polyisobutylene (PIB). The five polymer species differ from

each other in the degree of short side group branching, with this branching increasing from top to bottom of Figure 1, i.e., from PE to PIB.

An ideal choice of molecular weights for probing how these short branches affect the blend thermodynamics would have the site occupancy indices M_1 and M_2 for both species large enough, equal to each other, and identical for all the blends studied. Such an approach, however, leads in many cases to blends whose one-phase regions at 1 atm pressure are unrealistically diluted systems at astronomically high temperatures. Hence, we retain the convenient condition $M = M_1 = M_2$ but must admit variations in M for the different blends in order to describe sensible physical systems and for clarity in presenting the results. However, we attempt to maintain minimal variability in molecular weights.

The single microscopic interaction energy $\epsilon = \epsilon_{11} = \epsilon_{22} = \epsilon_{12}$ is taken as $\epsilon = 0.5k_BT_o$ ($T_o = 415.15$ K). While the absolute magnitudes of the calculated critical temperatures, excess volumes, or effective interaction parameters depend somewhat on the choice of ϵ, the general trends describing how these properties vary with blend architecture are fairly insensitive to the selected value of ϵ. Another adjustable parameter of the theory is the unit cell volume v_{cell}, which is assumed to be independent of the system and is chosen as $v_{cell} = 2.5477^3$ Å^3. The cell volumes for the actual polymer blends must vary slightly, but this assumed simplification follows from our goal of investigating the influence of the short chain branching. The use of a common cell volume is also consistent with the assumption of only one microscopic interaction energy ϵ.

A. Constant Pressure Spinodal Curves. The LCT constant pressure spinodal curves $T = T(\Phi_1)$ are generated from eq 2.7 and are presented in Figure 2a−e. Each of the individual portions of Figure 2 depicts a series of four binary blends having one common component, labeled as component 1, in order to illustrate the variation of the blend miscibility with the architecture of the second component (called species 2). As the degree of branching of polymer species 2 departs more from that of species 1, the blend miscibility is diminished and the upper critical solution temperature (UCST) phase diagram is shifted to higher temperatures. The four spinodals in each of Figure 2a−e are generated for blend samples with different molecular weights (as described in the figure caption). Otherwise, the spinodal curves for the less miscible systems (for instance, for PE/PIB or PE/P2B blends in Figure 2a) would appear for unphysically extremely high temperatures. This point may be understood by applying simple Flory−Huggins (FH) theory to Figure 2a, but ignoring for now the fact that, for our model, the FH $\chi = \epsilon_{ex}z/(2k_BT)$ is identically zero. Bearing in mind the above inadequacy and noting that our compressible theory generates a non-zero χ, FH theory for a symmetric blend yields the critical χ_c scaling as $\chi_c N = 2$, where N is the polymerization index. The range in M_i between the most miscible PE/PEP and the least miscible PE/PIB of Figure 2a is roughly 1 order of magnitude. Thus, a PE/PIB blend with $M = 2000$ would roughly be expected to yield a $T_c \approx 4000-5000$ K, well above a decomposition temperature. Similar considerations may be applied for the other blends depicted in Figure 2b−e. An examination of Figure 2a−e demonstrates clearly that blend compatability is enhanced by the presence of an architectural similarity between the monomers of the two blend components. For example, PIB and P2B chains have the most branched architectures of the five chains in Figure 1, and PIB mixes with P2B much better than either mixes with the least branched PE (see Figure 2e). On the other hand, P2B forms a homogeneous phase with PP more easily than even with PIB (see Figure 2d).

An important question immediately emerges from the observation of the spinodals in Figure 2a−e concerning the definition of a measure for this structural similarity and its eventual application to predicting blend miscibility. One commonly used measure of polymer miscibility is the fraction of end groups to total groups in the chain. However, this fraction of end groups is identical for the united atom models of P2B and PIB in Figure 1. Thus, the different LCT miscibilities of these two species lead us to consider other possible structural parameters that correlate with polyolefin blend compatibilities. Our earlier model LCT calculations[14] for incompressible binary blends provide a possible structural parameter. In particular, we have shown that the entropic portion $\chi_{eff}^{(S)}$ of χ_{eff} arises in the long chain ($M_1,M_2 \rightarrow \infty$), infinite pressure limit solely from the difference in the ratios $N_2^{(\alpha)}/M_\alpha$ for the two blending components,

$$\chi_{eff}^{(S)} = \frac{1}{z^2}\left[\frac{N_2^{(1)}}{M_1} - \frac{N_2^{(2)}}{M_2}\right]^2 \tag{3.1}$$

The combinatorial coefficient $N_2^{(\alpha)}$ in eq 3.1 denotes[12,14] the number of sequentially bonded sets of two bonds in a single polymer chain of species α and is, in general, a function of M_α and the chain architecture. (The table in the Appendix presents values of $N_2^{(\alpha)}$ appropriate to the five polyolefin structures in Figure 1.) The ratio $N_2^{(\alpha)}/M_\alpha$, on the other hand, depends almost entirely only on the chain structure, provided that M_α is not too small ($M_\alpha > 100$). Hence, we likewise consider the use for compressible blends of the quantity

$$r \equiv \left|[N_2^{(1)}/M_1 - N_2^{(2)}/M_2]\right| \tag{3.2}$$

as a possible measure of blend structural asymmetry and miscibility. The Appendix describes an approximate analytical representation of the stability conditions from the LCT and eq 2.10. This approximate treatment provides some additional impetus for our choice of r as a measure of blend miscibility.

Table 1 summarizes the computed r values along with the critical temperatures T_c for the phase separation of all ten compressible binary blends constructed from the polymer species of Figure 1. Since all these blends exhibit upper critical temperature phase diagrams, a higher critical temperature implies, in general, poorer miscibility (see Figure 2). Comparing Table 1 with Figure 2 demonstrates that blend miscibility diminishes with an increase of r, and there is a perfect correlation between the magnitudes of r and T_c. Of particular note are the nonintuitive cases of greater miscibility for P2B/PIB over P2B/PEP, for PP/PE over PP/PIB, or for PEP/PP over PE/PEP. These features accord with ordering of r's in Table 1.

The examples of Table 1 employ different site occupancy indices $M = M_1 = M_2$ for different blends in order to prevent the critical temperatures T_c from growing unreasonably for the less miscible systems. These choices for M do not, however, exert a practical impact on r or on the ordering of the binary blend critical temperatures. The values of $r^\infty \equiv r(M_1,M_2\rightarrow\infty)$ for the long chain limit ($M_1,M_2\rightarrow\infty$) are included in Table

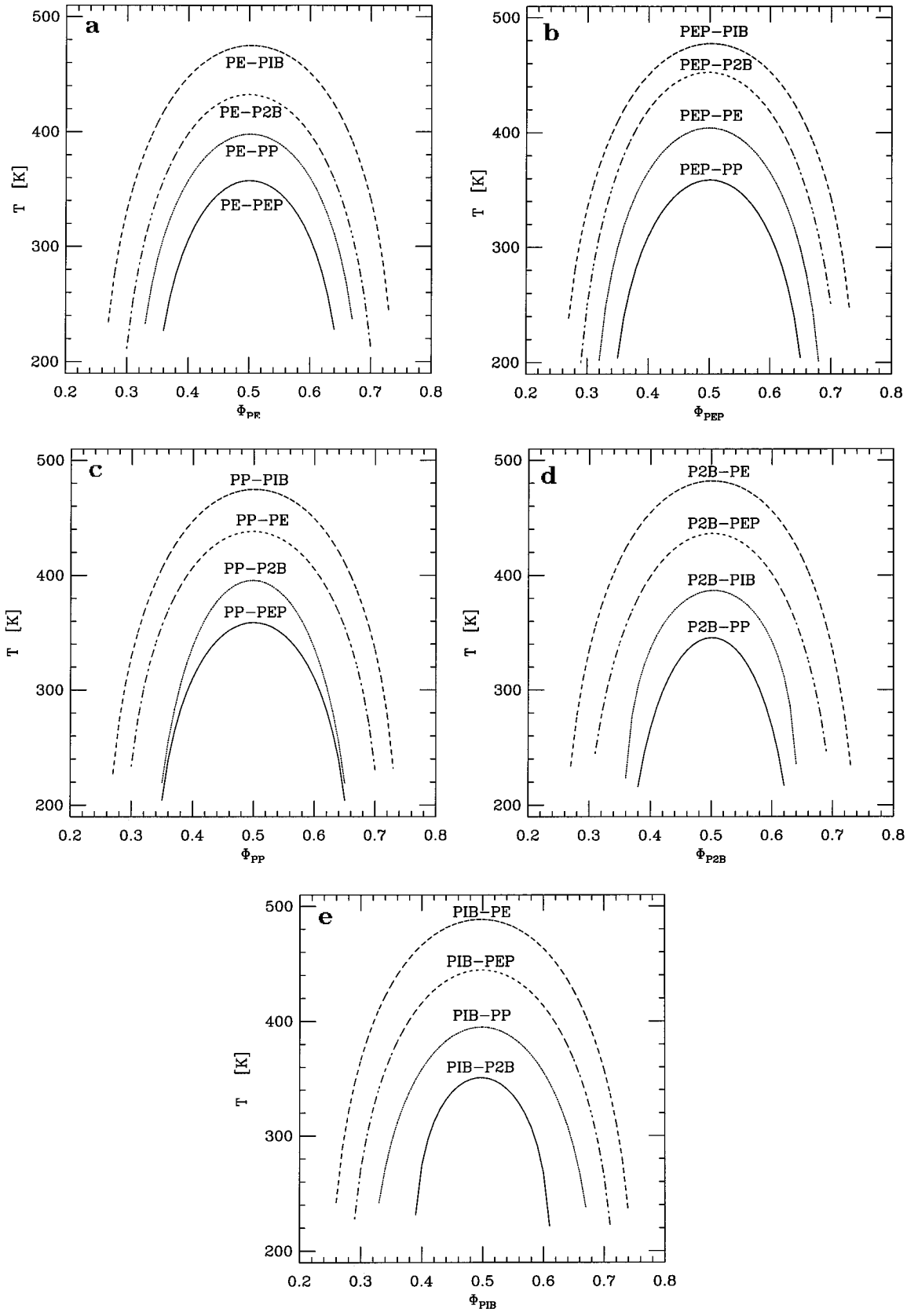

Figure 2. (a) LCT computations of spinodal curves at $P = 1$ atm for a series of polyolefin blends with PE as a common component. All curves are generated for the same microscopic interaction energy $\epsilon = \epsilon_{11} = \epsilon_{22} = \epsilon_{12} = 0.5k_BT_o$ ($T_o = 415.15$ K), but for different sets of site occupancy indices $M_1 = M_2 = 169$, 354, 754, and 2002 (top to bottom, respectively). (b) Same as Figure 2a but for a series of polyolefin blends with PEP as a common component. The curves from top to bottom are obtained for different sets of site occupancy indices $M_1 = M_2 = 312$, 992, 2102, and 4522, respectively. (c) Same as Figure 2a but for a series of polyolefin blends with PP as a common component. The curves from top to bottom are obtained for different sets of site occupancy indices $M_1 = M_2 = 541$, 793, 2914, and 4522, respectively. (d) Same as Figure 2a but for a series of polyolefin blends with P2B as a common component. The curves from top to bottom are obtained for different sets of site occupancy indices $M_1 = M_2 = 380$, 972, 1253, and 2812, respectively. (e) Same as Figure 2a but for a series of polyolefin blends with PIB as a common component. The curves from top to bottom are obtained for different sets of site occupancy indices $M_1 = M_2 = 173$, 297, 485, and 1213, respectively.

Table 1. Correlation of Blend Miscibility with the Blend Branching Parameter r, the Relative Excess Volume $V^e/(V_1 + V_2)$, and the SANS Effective Interaction Parameter χ_{eff} for Model Binary Polyolefin Blends at $P = 1$ atm

blend	M_1[b]	M_2	T_c, K	r[c]	r^∞	$[[V^e/(V_1 + V_2)] \times 10^{-3}]$[a]	χ_{eff}[a]
PE/PIB	173	173	488	0.7457	0.75	4.387	0.113×10^{-1}
PEP/PIB	312	313	477	0.5489	0.55	2.308	0.615×10^{-2}
PE/P2B	354	354	432	0.4972	0.5	1.852	0.510×10^{-2}
PP/PIB	484	485	395	0.4158	0.4167	1.306	0.354×10^{-2}
PE/PP	742	742	383	0.3329	0.3333	0.821	0.229×10^{-2}
PEP/P2B	902	902	365	0.2993	0.3	0.659	0.187×10^{-2}
P2B/PIB	1212	1213	351	0.2502	0.25	0.593	0.135×10^{-2}
PE/PEP	1972	1972	340	0.1998	0.2	0.290	0.829×10^{-3}
PP/P2B	2782	2782	328	0.1664	0.1667	0.209	0.608×10^{-3}
PEP/PP	4342	4342	311	0.1333	0.1333	0.132	0.366×10^{-3}

[a] Quantity calculated for a symmetric blend ($\Phi_1 = \Phi_2 = 0.5$) at $T = 500$ K. [c] The blend branching parameter r is given by eq 3.2. The long chain limit $r^\infty \equiv r(M_1, M_2 \rightarrow \infty)$. [b] M_α is the site occupancy index for polymer species α and T_c designates the critical temperature for the blend phase separation.

1 to indicate the proximity of the chosen M to this limit. As mentioned above, an adequate comparison of miscibility for two blends formally requires the same M for both of them. Comparing the compatibility of two different UCST blends with different $M = M_1 = M_2$ is justified only when the blend that exhibits the higher critical temperature T_c has the lower molecular weights because its T_c would only grow further with increasing M. All the blends illustrated in Figure 2 and Table 1 satisfy this condition. Of course, a large increase in M for a more miscible blend would increase its T_c above that for a much lower M, less miscible blend. Thus, Table 1 is also constructed with the requirement that blends with *higher* T_c must also involve *lower* values for M.

The presence of the second-order energy (ϵ^2) terms in eq 2.1 represents contributions from nonrandom mixing. When the spinodals are recalculated (see Appendix) without these ϵ^2 terms, the resultant errors in the determination of T_c range from 15 K for the most miscible PEP/PP to 45 K for the least miscible PE/PIB system. Hence, nonrandom mixing contributions are more significant for the more immiscible blends. In spite of the errors incurred by introducing a more approximate random mixing assumption into the LCT theory, the computed critical temperatures preserve the same order as illustrated in Table 1 for the full nonrandom mixing LCT theory.

In contrast to systems exhibiting a lower critical solution temperature (LCST) phase diagram where an applied pressure favors[16,17] blend miscibility, an increase of pressure renders the binary UCST polyolefin blends less miscible (for $\epsilon_{ex} = 0$). Figure 3 shows a sample prediction of such behavior by the LCT for a PEP/PP binary blend. Similar qualitative trends are found for the other model polyolefin blends constructed from the polymer species of Figure 1. Our ability to describe the pressure dependence of phase diagrams[17] is one useful bonus from using a more realistic compressible model.

B. Excess Volume for Binary Polyolefin Blends at $P = 1$ atm. The non-zero excess volume ΔV of binary blends is one important blend property that can be computed only by treating the blends as compressible systems. Equation 2.14 represents the relative excess volume $\Delta V/(V_1 + V_2)$ as a function of the blend composition Φ_1, the void volume fraction ϕ_v in the blend, and the analogous quantities $\phi_v^{(1)}$ and $\phi_v^{(2)}$ for the pure component 1 and 2 melts. These three free volume fractions are obtained from the appropriate LCT equations of state. Because our model involves only one interaction energy parameter ϵ, the excess volume is expected to be positive, with its magnitude governed solely by the monomer structures of the two blend components.

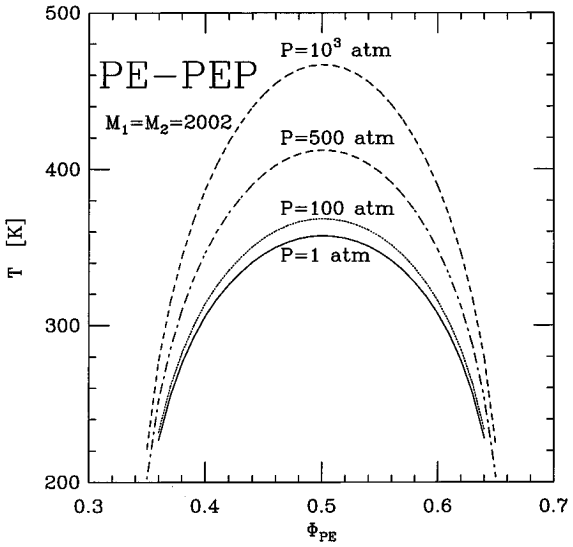

Figure 3. LCT computations of spinodal curves for a PE/PEP blend at different pressures as indicated in the figure. The single interaction energy parameter is $\epsilon = 0.5 k_B T_o$ ($T_o = 415.15$ K).

Parts a and b of Figure 4 present a few examples of the excess volume calculated over the whole range of blend compositions for two series of blends having, respectively, PP and PE as the common components. The architectural similarity of the blend components leads to a small excess volume (see Figure 4b for PE/PEP), while an increasing structural asymmetry between both polymer species yields a large $V^e/(V_1 + V_2)$ (see the same figure for PE/PIB). Comparing both figures with the spinodal curves of Figure 2c and Figure 2a for the same series of systems demonstrates the existence of a correlation between the blend miscibility (or the critical temperature T_c for the phase separation) and the excess volume. Such a correlation is additionally confirmed by identical calculations for the other binary blends constructed from the chains of Figure 1. These computations are summarized in Table 1, which includes the values of $V^e/(V_1 + V_2)$ for the single composition $\Phi_1 = 0.5$. A poorer miscibility correlates with a higher r and also implies a larger excess volume since the less miscible polymer chains have more asymmetrical side groups which, in turn, need more space to mix in a stable homogeneous phase. The computed relative excess volumes are practically insensitive to the molecular weights M over the ranges considered, so the use of different M for the different blends is irrelevant to $V^e/(V_1 + V_2)$.

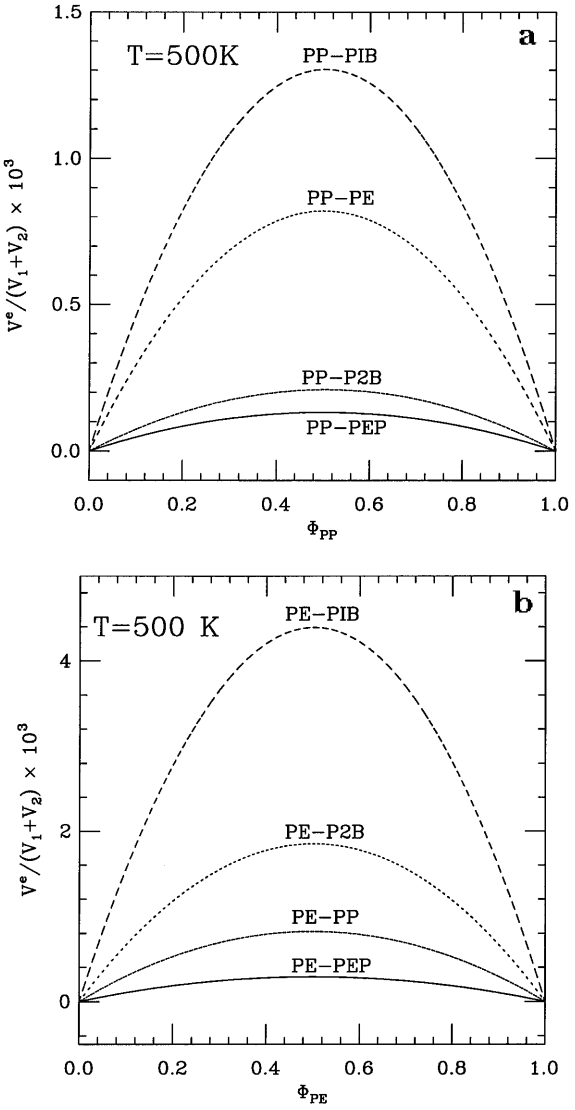

Figure 4. (a) LCT computations of the relative excess volume $V^e/(V_1 + V_2)$ at $P = 1$ atm and $T = 500$ K for a series of polyolefin blends with PP as a common component. The single interaction energy parameter is $\epsilon = 0.5k_BT_o$ ($T_o = 415.15$ K). The curves from top to bottom are obtained for different sets of site occupancy indices $M_1 = M_2 = 541$, 793, 2914, and 4522, respectively. (b) Same as Figure 4a, but for a series of polyolefin blends with PE as a common component. The curves from top to bottom are obtained for $M_1 = M_2 = 169$, 354, 754, and 2002, respectively.

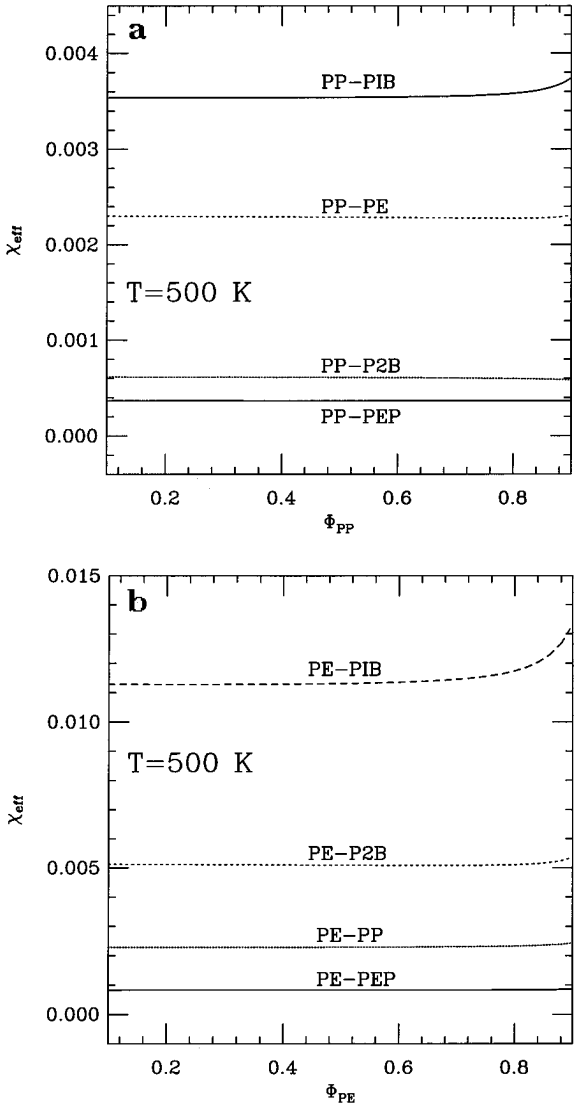

Figure 5. (a) LCT computations of the effective interaction parameter χ_{eff} at $P = 1$ atm and $T = 500$ K for a series of polyolefin blends with PP as a common component. The single interaction energy parameter is $\epsilon = 0.5k_BT_o$ ($T_o = 415.15$ K). The curves from top to bottom are obtained for $M_1 = M_2 = 541$, 793, 2914, and 4522, respectively. (b) Same as Figure 5b, but for a series of polyolefin blends with PE as a common component. The curves from top to bottom are obtained for $M_1 = M_2 = 169$, 354, 754, and 2002, respectively.

C. SANS Effective Interaction Parameter χ_{eff} for Binary Polyolefin Blends at $P = 1$ atm. As mentioned earlier, the LCT computations of the effective interaction parameter χ_{eff} are performed with the commonly used defintion of eq 2.11. First of all, the computed χ_{eff} is practically independent of composition (see Figure 5a,b), except for the occurrence of a slight parabolic upward curvature at high Φ_1 ($\Phi_1 > 0.8$) and low M. The absence of a composition dependence for χ_{eff} stems from the presence of only one interaction energy $\epsilon = \epsilon_{11} = \epsilon_{22} = \epsilon_{12}$ and, therefore, of an identically vanishing exchange energy ϵ_{ex}. A nontrivial composition dependence $\chi_{eff}(\Phi_1)$ is anticipated for some of these systems when lifting the assumption of a common ϵ.

Table 1 also contains the computed effective interaction parameter χ_{eff} at $T = 500$ K, $P = 1$ atm, and $\Phi_1 = 0.5$ for the series of ten model binary blends. These χ_{eff} suggest the existence of a correlation between blend miscibility and the effective interaction parameter similar to that found for the excess volumes $V^e/(V_1 + V_2)$ and for the structural parameter r. Both χ_{eff} and $V^e/(V_1 + V_2)$ decrease when the miscibility improves. Such a behavior of χ_{eff} confirms the validity of the traditional interpretation in which a smaller χ_{eff} implies a more negative free energy of mixing and a better compatibility of the two blend species. The fact that the χ_{eff} values in Table 1 are computed for different M does not affect the ordering χ_{eff} with T_c since χ_{eff} is found to grow slightly (by only a few percent) with an increase of M. Hence, the χ_{eff} for the lower molecular weight blends in Table 1 would only slightly increase if the same, highest molecular weights ($M = 4342$) could be used in all calculations.

The conventional analysis of SANS scattering data for χ_{eff} involves the separation of the temperature independent portion of χ_{eff}, called the "entropic" part χ_s, from the temperature dependent contribution, called the "enthalpic" part χ_h, following the usual empirical relation,

Table 2. Comparison of the "Entropic" and the "Enthalpic" Portions of the Effective Interaction Parameter χ_{eff} for Model Binary Polyolefin Blends at $P = 1$ atm

blend	M_1	M_2	T_c, K	χ_s,[a] K	χ_h[a]	$\chi_h^{(T)} \equiv \chi_h/(T_c + 25\ K)$	$\chi_s/\chi_h^{(T)}$
PE/PIB	173	173	488	-0.3248×10^{-3}	5.8188	0.1134×10^{-1}	−0.029
PEP/PIB	312	313	477	0.4560×10^{-3}	2.8443	0.5666×10^{-2}	0.080
PE/P2B	354	354	432	0.1877×10^{-2}	1.6352	0.3578×10^{-2}	0.52
PP/PIB	484	485	395	0.1840×10^{-2}	0.9062	0.2158×10^{-2}	0.85
PE/PP	742	742	383	0.1356×10^{-2}	0.5150	0.1262×10^{-2}	1.07
PEP/P2B	902	902	365	0.1327×10^{-2}	0.3259	0.8358×10^{-3}	1.59
P2B/PIB	1212	1213	351	0.1049×10^{-2}	0.2119	0.5635×10^{-3}	1.86
PE/PEP	1972	1972	340	0.6486×10^{-3}	0.1249	0.3423×10^{-3}	1.89
PP/P2B	2782	2782	328	0.5463×10^{-3}	0.0569	0.1611×10^{-3}	3.39
PEP/PP	4342	4342	311	0.3249×10^{-3}	0.0424	0.1262×10^{-3}	2.58

[a] Quantity calculated for a symmetric blend ($\Phi_1 = \Phi_2 = 0.5$) using a least squares fit of χ_{eff} vs $1/T$ in the temperature range between T_c and $T_c + 50$ K, where T_c designates the critical temperature for the blend phase separation as given in Table 1.

$$\chi_{eff} = \chi_s + \chi_h \frac{1}{T} \tag{3.3}$$

The LCT calculations for the temperature dependence of χ_{eff} provide important information concerning how these entropic and enthalpic portions of χ_{eff} vary for polyolefin blends. The χ_s and χ_h are determined for each of the blends in Table 1 using the temperature range between T_c and $T_c + 50$ K, for $\Phi_1 = 0.5$ and $P = 1$ atm. Table 2 summarizes both portions of χ_{eff} as well as the enthalpic contribution $\chi_h^{(T)} \equiv \chi_h/(T_c + 25\ K)$ calculated at a temperature $T = T_c + 25$ K for all ten blends of Table 1. The enthalpic contribution χ_h decreases monotonically with improved blend miscibility (i.e., with lower T_c), while the ratio of χ_s to $\chi_h^{(T)}$ increases quite sharply. Hence, the less miscible blends have their interaction parameter χ_{eff} mostly of enthalpic origin, whereas the χ_{eff} for highly miscible blends become dominated by the entropic portion. This observation matches an intuitive picture in which the entropic contribution to χ_{eff} arises solely from packing constraints, while the enthalpic one is a consequence of both packing- and interaction-induced correlations. The numerical results of Table 2 depend on the temperature range over which the least squares fit to eq 3.3 is applied, but the general trends remain unchanged for other ranges, as explained below. The entropic portion χ_s of χ_{eff} in Table 2 displays a maximum, while the enthalpic portion χ_h monotonically decreases with the blend miscibility. If eq 3.3 is applied using a common temperature range between 500 and 550 K for all the blends, we obtain the same qualitative behavior for the χ_h, but no systematic variation is found for χ_s (which becomes negative and exhibits an oscillatory character with several extrema) although χ_s/χ_h still increases substantially with blend miscibility. This observation, as well as the occurrence of different signs for χ_s in the different temperature ranges used, illustrates the rather complex character of χ_s and suggests caution in its interpretation for this simple model with $\epsilon_{ex} = 0$.

IV. Discussion

Our LCT calculations employ a generalized united atom lattice model for polyolefins to study the effects of short chain branching on blend miscibility and other thermodynamic properties [such as the SANS effective interaction parameter χ_{eff} and the relative excess volume $V^e/(V_1 + V_2)$] of binary polyolefin blends. This goal is accomplished by using a simplified model, in which all united atom units interact with the same microscopic energy ϵ. This single energy model yields liquid densities at ambient pressures and is, therefore, far superior to the commonly used athermal limit model (with all interactions vanishing) that requires elevated pressures for producing liquid densities. On the other hand, the absence of interaction asymmetries for the individual C, CH, CH_2, or CH_3 united atom groups of polyolefin chains represents an evident approximation since these groups must interact with different energies, in spite of their similar chemical structures.[18] The next simplest molecular level model would contain at least three independent average interaction energies ϵ_{11}, ϵ_{22}, and ϵ_{12} which are ascribed to given monomer pairs. Introducing this feature into the LCT calculations is straightforward (see our previous applications[13−17]) and is deferred to a future study which will consider detailed quantitative comparisons with experiment. The present single interaction energy model is used to focus solely on the general but poorly understood phenomenon[22] of how blend miscibility and other thermodynamic properties are qualitatively affected by short chain branching.

It is no surprise that the LCT computations find the blend miscibility to vary with the monomer structures of the two blend components. Blends with higher degrees of structural asymmetry are more poorly miscible, while blends whose side groups are more "similar" exhibit better compatibility. Of more significance is addressing the question of devising a quantitative description for this phenomenon and, in particular, devising a quantitative measure of the morphological similarity in chain architecture that would enable the prediction and comparison of blend miscibilities. The LCT computations display the purely theoretical blend branching degree parameter r, defined by eq 3.2, as an appropriate quantity for such a purpose. Additional correlations with blend miscibility are the excess volume V^e and the effective interaction parameter χ_{eff}. Although these predictions are based on the simplified, single energy parameter model, they can be treated at least as a first-order estimation until we have more elaborate treatments with monomer dependent interaction energies. The computations of r are trivial compared to those for the spinodal curves. The evaluation of r requires only a knowledge of the geometrical factors $N_2^{(1)}$ and $N_2^{(2)}$ for the two blend components (see Table 3 for the values appropriate to the chains in Figure 1). Smaller differences in $N_2^{(\alpha)}/M_\alpha$ between the two blend components yield a smaller branching degree r which, in turn, favors blend miscibility. This branching parameter r is more general than a commonly used miscibility index constructed as the ratio of end CH_3 groups to total CH_n groups. The latter structural parameter does not distinguish between PIB and P2B, whereas the parameter r correctly correlates with their differing blend miscibilities.

Table 3. Combinatorial Factors for the Model Polyolefin Chains of Figure 1

polymer	N_1	N_2	N_3	$N_\perp$	$N_{1,1}$	$N_{1,2}$
PE	N^a	$N-1$	$N-2$	0	$(N-1)(N-2)/2$	$(N-2)(N-3)$
PEP	$(5N-1)/4$	$^3/_2(N-1)$	$(3N-7)/2$	$(N-1)/4$	$(N-1)(25N-53)/32$	$(15/8)N^2-9N+89/8$
PP	$^3/_2N$	$2N-1$	$2(N-2)$	$N/2$	$(N-2)(9N-4)/8$	$(N-2)(3N-5)$
P2B	$2N-1$	$3(N-1)$	$4(N-2)$	$N-1$	$2(N-1)(N-2)$	$2(N-2)(3N-7)$
PIB	$2N$	$^7/_2(N-1)$	$3(N-2)$	$2N$	$(N-2)(4N-1)/2$	$7(N-1)(N-2)$

[a] N is the number of bonds in the chain backbone. The site occupancy index M (the total number of sites occupied by a single chain) is equal to N_1+1 for all the polymer chain architectures in Figure 1.

Another suggested[6] defining measure of the blend structural asymmetry involves the use in eq 3.2 of the Kuhn lengths,

$$l_\alpha = [6R_{G,\alpha}{}^2/N_\alpha]^{1/2} \tag{4.1}$$

instead of the geometrical coefficients $N_2^{(\alpha)}/M_\alpha$. The radius of gyration for a chain of a given species α is defined as,

$$R_{G,\alpha}{}^2 \equiv \frac{1}{N_\alpha{}^2}\sum_{i<j}\langle \mathbf{r}_{ij}\rangle^2 \tag{4.2}$$

where the summation indices i and j run over all distinguishable pairs of subunits occupying single lattice sites and where N_α denotes the number of these pairs. The exact computation of $R_{G,\alpha}{}^2$ for the structured monomer chains is, unfortunately, extremely tedious. Thus, we have employed an approximate non-self-reversing random walk model for the chain conformations, a model that accords roughly with the conformational properties deduced from simulations and observations for single chains in the melt. To leading order in z^{-1}, this model enables us to assume that only adjacent bond vectors $\mathbf{r}_{ij}$ are correlated if these bonds are attached to a common lattice site. However, the computed Kuhn lengths to order z^{-1} are found mostly to be independent of the chain architectures (although they should differ in higher orders). Thus, these l_α do not scale as the geometrical parameter r, and the differences in computed Kuhn lengths do not correlate with blend miscibilities to order z^{-1}. Perhaps, when the LCT is extended to include explicit trans−gauche energy differences, similar model system computations would display the partial correlations with blend miscibility that are found by Graessley and co-workers.[2,4]

The analytical formula for the critical temperature T_c is rather lengthy. A simpler estimation for T_c is obtained by invoking a random mixing approximation within LCT, where the nonnegligible second-order contributions in the interaction energies are ignored. The analysis is provided in the Appendix. The parameter $(r/z)^2$ figures prominently in eq A.1 along with several other combinatorial factors associated with the monomer structures. Since the ratio r exhibits an excellent correlation with blend miscibility, we have not considered possible correlations with the other quantities in eqs A.4a−A.4b. The nonrandom mixing contributions to T_c increase in importance as the blend miscibility diminishes. Thus, the least miscible PE/PIB blend yields T_c differing by almost 50 K between the random and nonrandom mixing calculations.

Blend miscibility grows monotonically with a decreasing branching degree parameter r, and miscibility is also correlated directly with the excess volume $V^e/(V_1+V_2)$ and with the SANS effective interaction parameter χ_{eff}. The examples in Table 1 demonstrate that the poorest miscibility implies the highest excess volume and the highest effective interaction parameter and that these two quantities monotonically diminish as the miscibility becomes more favorable, achieving a minimum for the most compatible PEP/PP blend. The positive sign of $V^e/(V_1+V_2)$ stems from the absence of an energetic preference ($\epsilon_{ex}=0$) that arises as a consequence of using a single interaction energy model. The existence of similar correlations to those illustrated in Table 1 can be anticipated for more general models with three independent $\epsilon_{\alpha\beta}$.

One of the main controversies concerning binary polyolefin blends lies in the origin of the SANS effective interaction parameter χ_{eff}. While the theory of Bates, Fredrickson, et al.[6] describes the χ_{eff} for polyolefin blends as a quantity arising almost entirely from architectural and flexibility differences between the two components, the recent PRISM analysis of Singh and Schweizer[7] suggests that the enthalpic portion χ_h of χ_{eff} is much more important than the purely entropic part χ_s. On the other hand, our LCT calculations for a single interaction energy model indicate that except for the very immiscible polyolefin blends (such as PE/PIB or PEP/PIB), both portions of χ_{eff} are relevant and comparable to each other, with an increasing dominance of the entropic part χ_s over the enthalpic contribution χ_h/T when the blend miscibility improves. This observation extends the PRISM prediction of Singh and Schweizer[7] by relating the relative magnitudes of χ_s and χ_h to the monomer structures of the two blend components and to the blend miscibility. Both the LCT and PRISM theories, in contrast to the approach of Bates, Fredrickson, et al.[6] treat polyolefins as compressible systems, and this is probably the reason for their similar conclusions on the relevance of χ_h. Our many examples with the LCT demonstrate[13−17,23] that polymer blend compressibility is a crucial ingredient of the meaningful thermodynamic description[9] of these systems. Ignoring the presence of compressibility can lead to serious oversimplifications in the theoretical predictions of blend thermodynamics.

The LCT is a mean field theory, albeit very sophisticated, and ignores the presence of long range fluctuations, the feature used by Bates, Fredrickson, et al.[6] to predict a relation between Kuhn length asymmetry and blend miscibility. Since the χ_{eff} determined by Bates, Fredrickson, et al. is proportional to the cube of a cutoff parameter on **k**-space integrals, 99% of the contribution emerges from the range between l_α and $5l_\alpha$. Equating l_α to the lattice constant suggests that the dominant contributions are indeed of short range, as included in the LCT.

The SANS experimental data of Graessley et al.[1−4] for random copolymer binary polyolefin blends have recently been analyzed in terms of the solubility parameter theory. In spite of some successes, this type of analysis is not universal and fails to explain the effective interaction parameters for LCST systems. The solubility parameters are defined in ref 3 by

$$\delta_{PVT} = \left(\frac{T\alpha}{\beta}\right)^{1/2} \tag{4.3}$$

where the thermal expansion coefficient α and the compressibility coefficient β are obtained from the equations of state for pure components. The definition in eq 4.3 explicitly treats the pure melts as compressible, but the resultant solubility parameters are inserted into an *incompressible model* for χ_{eff}. Such an incompressible model misses the importance of the enthalpic contributions found to be relevant by both LCT and PRISM computations.

Solubility parameters may also be computed from eq 4.3 and the LCT equations of state for the pure components. These LCT solubility parameters are almost identical for all ten blends and therefore fail to correlate with the LCT blend miscibilities. More decisive tests on the utility of the solubility parameter theory for understanding blend miscibility may require the use of more realistic models for polyolefin blends. For instance, consider the next level model of compressible blends with three independent averaged interaction energies ϵ_{11}, ϵ_{22}, and ϵ_{12} for the united atom subunits of the different homopolymers. The LCT for this model already provides insight into the origin of what Graessley et al.[2] call the excess portion of χ_{eff} that is associated with deviations from solubility parameter theory. The LCT free energy expression contains terms with the differences $\epsilon_{11} - \epsilon_{22}$, $\epsilon_{11} - \epsilon_{12}$, etc. When the common representation of the pure melt reduced temperatures is introduced as $T_1^* \sim \epsilon_{11}$ and $T_2^* \sim \epsilon_{22}$ and the common combining rule $\epsilon_{12} = \sqrt{\epsilon_{11}\epsilon_{22}} \sim \sqrt{T_1^* T_2^*}$ is invoked, these additional interaction terms scale as $T_1^* - T_2^*$, $\sqrt{T_1^*}(\sqrt{T_1^*} - \sqrt{T_2^*})$, etc. and appear only because the system is compressible. Graessley and co-workers note[4] a marked increase in deviations from solubility parameter theory with increasing $|T_1^* - T_2^*|$, a feature that presumably arises from these compressible system interaction terms. Indeed, some computations[15] with a three interaction energy model have already produced closed loop phase diagrams, but more extensive computations are required with the energetic parameters determined laboriously from empirical data.

Acknowledgment. This research is supported, in part, by NSF DMR Grant No. 92-23804. We thank Bill Graessley for suggesting the excess volume as a candidate that may correlate well with blend miscibilities.

Appendix: Random Mixing LCT Estimation of the Critical Temperature T_c for the Phase Separation of Model Polyolefin Blends

Ignoring the second-order energy terms in eq 2.1 and assuming that the maximum of the spinodal curve occurs exactly at $\Phi_1 = 0.5$ enable us to obtain a simple random mixing model estimation for the critical temperature T_c as

$$\frac{T_c}{T_o} \approx \frac{\epsilon}{k_B T_o} \frac{-X_1 \pm \sqrt{X_1^2 - 4X_2X_3}}{2X_2} \tag{A1}$$

where $T_o = 415.15$ K as in section III,

$$X_1 = A^2 + B\left[\frac{1}{\phi_v} - \frac{2}{z}m^2 + \frac{2}{z^2}\{(\lambda_1 + \lambda_2)m - (1/4)[\kappa_1 + \kappa_2]^2 - m^2(1 - \phi_v)[6(\gamma_1 + \gamma_2) + 8m + 12m^2(1 - \phi_v)]\}\right] \tag{A2a}$$

$$X_2 = 2AC + B\left[-z - 2m + 6m\phi_v + \frac{1}{z^2}\{(\lambda_1 + \lambda_2)(1 - 3\phi_v) - 4(\gamma_1 + \gamma_2)m[1 - 6\phi_v + 6\phi_v^2] + 24m^2(1 - \phi_v)[3m + 2\phi_v - 4m\phi_v] - 80m^3(1 - \phi_v)^3 - 8m^2\}\right] \tag{A2b}$$

$$X_3 = C^2 \tag{A2c}$$

with

$$A \equiv -\frac{1}{z^2}[2(\lambda_1 - \lambda_2)m - 8(\gamma_1 - \gamma_2)m^2(1 - \phi_v) - \kappa_1^2 + \kappa_2^2] \tag{A3a}$$

$$B \equiv 2\left(\frac{r}{z}\right)^2 - \frac{4}{M(1 - \phi_v)} \tag{A3b}$$

$$C \equiv \frac{1}{z}[2(\lambda_1 - \lambda_2)\phi_v - 4(\gamma_1 - \gamma_2)m\phi_v(2 - 3\phi_v)] \tag{A3c}$$

All the quantities λ_α, γ_α, and κ_α in eqs A.2 and A.3 are defined in terms of the structure-dependent geometrical coefficients[12] $\{N_i\}$ and site occupancy indices M_α as

$$\lambda_\alpha \equiv [2N_2^{(\alpha)} + N_3^{(\alpha)} + 3N_\perp^{(\alpha)} + 2(N_{1,2}^{(\alpha)} - N_1^{(\alpha)}N_2^{(\alpha)}M_\alpha)]/M_\alpha \tag{A4a}$$

$$\gamma_\alpha \equiv [N_{1,1}^{(\alpha)} - (1/2)(N_1^{(\alpha)})^2 M_\alpha]/M_\alpha \tag{A4b}$$

$$\kappa_\alpha \equiv N_2^{(\alpha)}/M_\alpha \tag{A4c}$$

and

$$r \equiv |\kappa_1 - \kappa_2| \qquad m \equiv N_1^{(\alpha)}/M_\alpha = 1 - 1/M \qquad M_1 = M_2 = M$$

The coefficients $N_1^{(\alpha)}$, $N_2^{(\alpha)}$, $N_3^{(\alpha)}$, $N_\perp^{(\alpha)}$, $N_{1,1}^{(\alpha)}$, and $N_{1,2}^{(\alpha)}$ represent the number of ways of selecting various combinations of bonds in a single polymer chain of species α. The definitions of $\{N_i\}$ are presented in refs 12 and 14 along with the explicit values for twelve vinyl monomer structures, but for convenience Table 3 summarizes these combinatorial factors $\{N_i\}$ for all five model polyolefin chains of Figure 1.

References and Notes

(1) Krishnamoorti, R.; Graessley, W. W.; Balsara, N. P.; Fetters, L. J.; Lohse, D. J. *Macromolecules* **1994**, *27*, 3073. Graessley, W. W.; Krishnamoorti, R.; Balsara, N. P.; Butera, R. J.; Fetters, L. J.; Lohse, D. J.; Schulz, D. N.; Sisano, J. A. *Macromolecules* **1994**, *27*, 3896.
(2) Graessley, W. W.; Krishnamoorti, R.; Reicchart, G. C.; Balsara, N. P.; Fetters, L. J.; Lohse, D. J. *Macromolecules* **1995**, *28*, 1260.
(3) Krishnamoorti, R.; Graessley, W. W.; Fetters, L. J.; Garner, R. J.; Lohse, D. J. *Macromolecules* **1995**, *28*, 1252.
(4) Krishnamoorti, R.; Graessley, W. W.; Dee, G. T.; Walsh, D. J.; Fetters, L. J.; Lohse, D. J. Preprint.
(5) Rowlinson, J. S.; Swinton, F. L. *Liquids and Liquid Mixtures*, 3rd ed.; Butterworth: London, 1982.

(6) Bates, F. S.; Schultz, M. F.; Rosedale, J. H.; Almdal, K. *Macromolecules* **1992**, *25*, 5547. Gehlsen, M. D.; Bates, F. S. *Macromolecules* **1994**, *27*, 3611. Bates, F. S.; Fredrickson, G. H. *Macromolecules* **1994**, *27*, 1065. Fredrickson, G. H.; Liu, A. J.; Bates, F. S. *Macromolecules* **1994**, *27*, 2503. Fredrickson, G. H.; Liu, A. J. *J. Polym. Sci., Polym. Phys.* **1995**, *33*, 1203.
(7) Singh, C.; Schweizer, K. S. *J. Chem. Phys.* **1995**, *103*, 5814.
(8) Dudowicz, J.; Freed, K. F. *Macromolecules* **1990**, *23*, 1519.
(9) Sanchez, I. C.; Lacombe, R. H. *Macromolecules* **1978**, *11*, 1145.
(10) Foreman, K. W.; Freed, K. F. *J. Chem. Phys.* **1995**, *102*, 4663.
(11) Dudowicz, J.; Freed, K. F.; Madden, W. G. *Macromolecules* **1990**, *23*, 4803.
(12) Dudowicz, J.; Freed, K. F. *Macromolecules* **1991**, *24*, 5074.
(13) Dudowicz, J.; Freed, M. S.; Freed, K. F. *Macromolecules* **1991**, *24*, 5096.
(14) Dudowicz, J.; Freed, K. F. *Macromolecules* **1991**, *24*, 5112.
(15) Freed, K. F.; Dudowicz, J. *Theor. Chim. Acta* **1992**, *82*, 357.
(16) Dudowicz, J.; Freed, K. F. *Macromolecules* **1993**, *26*, 213.
(17) Dudowicz, J.; Freed, K. F. *Macromolecules* **1995**, *28*, 6625.
(18) Toxvaerd, S. *J. Chem. Phys.* **1990**, *93*, 4290. Jorgensen, W. L. *J. Am. Chem. Soc.* **1981**, *103*, 335; Mondello, M.; Grest, G. S. *J. Chem. Phys.* **1995**, *103*, 7156.
(19) Flory, P. J. *Discuss. Faraday Soc.* **1970**, *49*, 7.
(20) Sanchez, I. C. *Macromolecules* **1991**, *24*, 908.
(21) Dudowicz, J.; Lifschitz, M.; Freed, K. F.; Douglas, J. F. *J. Chem. Phys.* **1993**, *99*, 4804.
(22) Chai, Z.; Sun, R.; Li, S.; Karasz, F. E. *Macromolecules* **1995**, *28*, 2297. Barham, P. J.; Hill, M. J.; Golbeck-Wood, G. *Polymer* **1993**, *34*, 2871. Hill, M. J.; Barham, P. J. *Polymer* **1993**, *34*, 2975.
(23) Freed, K. F.; Dudowicz, J. *Trends Polym. Sci.* **1995**, *3*, 248.

MA951062Q